Original Article

pISSN 2234-7518 • eISSN 2005-372X
https://doi.org/10.4041/kjod.2022.52.2.85

THE KOREAN JOURNAL of ORTHODONTICS

Characterization of facial asymmetry phenotypes in adult patients with skeletal Class III malocclusion using three-dimensional computed tomography and cluster analysis

Sang-Woon Ha[a]
Su-Jung Kim[b]
Jin-Young Choi[c]
Seung-Hak Baek[d]

[a]Department of Orthodontics, School of Dentistry, Seoul National University, Seoul, Korea
[b]Department of Orthodontics, Kyung Hee University School of Dentistry, Seoul, Korea
[c]Department of Oral and Maxillofacial Surgery, School of Dentistry, Seoul National University, Seoul, Korea
[d]Department of Orthodontics, School of Dentistry and Dental Research Institute, Seoul National University, Seoul, Korea

Objective: To classify facial asymmetry (FA) phenotypes in adult patients with skeletal Class III (C-III) malocclusion. **Methods:** A total of 120 C-III patients who underwent orthognathic surgery (OGS) and whose three-dimensional computed tomography images were taken one month prior to OGS were evaluated. Thirty hard tissue landmarks were identified. After measurement of 22 variables, including cant (°, mm), shift (mm), and yaw (°) of the maxilla, maxillary dentition (Max-dent), mandibular dentition, mandible, and mandibular border (Man-border) and differences in the frontal ramus angle (FRA, °) and ramus height (RH, mm), K-means cluster analysis was conducted using three variables (cant in the Max-dent [mm] and shift [mm] and yaw [°] in the Man-border). Statistical analyses were conducted to characterize the differences in the FA variables among the clusters. **Results:** The FA phenotypes were classified into five types: 1) non-asymmetry type (35.8%); 2) maxillary-cant type (14.2%; severe cant of the Max-dent, mild shift of the Man-border); 3) mandibular-shift and yaw type (16.7%; moderate shift and yaw of the Man-border, mild RH-difference); 4) complex type (9.2%; severe cant of the Max-dent, moderate cant, severe shift, and severe yaw of the Man-border, moderate differences in FRA and RH); and 5) maxillary reverse-cant type (24.2%; reverse-cant of the Max-dent). Strategic decompensation by pre-surgical orthodontic treatment and considerations for OGS planning were proposed according to the FA phenotypes. **Conclusions:** This FA phenotype classification may be an effective tool for differential diagnosis and surgical planning for Class III patients with FA.
[Korean J Orthod 2022;52(2):85-101]

Key words: Facial asymmetry, Class III malocclusion, Cluster analysis

Received June 17, 2021; Revised July 22, 2021; Accepted September 1, 2021.

Corresponding author: Seung-Hak Baek.
Professor, Department of Orthodontics, School of Dentistry and Dental Research Institute, Seoul National University, 101, Daehak-ro, Jongno-gu, Seoul 03080, Korea.
Tel +82-2-2072-3952 **e-mail** drwhite@unitel.co.kr

How to cite this article: Ha SW, Kim SJ, Choi JY, Baek SH. Characterization of facial asymmetry phenotypes in adult patients with skeletal Class III malocclusion using three-dimensional computed tomography and cluster analysis. Korean J Orthod 2022;52:85-101.

INTRODUCTION

The etiology of facial asymmetry (FA) includes genetic or congenital malformations, acquired or developmental deformities, environmental factors including habits or trauma, and functional deviations.[1] Piao et al.[2] reported that the prevalence of FA in Korean orthodontic patients was the highest in skeletal Class III malocclusion, followed by skeletal Class I and Class II malocclusions (16.6%, 10.1%, 6.9%, p < 0.001), despite data from a single dental hospital.

FA has been diagnosed using facial photographs, posteroanterior (PA) cephalograms, or submentovertex projections. Although facial photographs can provide an intuitive impression of FA, it is difficult to accurately measure the amount of asymmetry. PA cephalograms and/or submentovertex projections are useful for diagnosis and orthognathic surgical planning of oral and maxillofacial deformities. However, these modalities have limitations due to magnification, projection errors, and two-dimensional (2D) assessments of the three-dimensional (3D) structures.[3] Therefore, the use of 3D computed tomography (3D-CT) or cone-beam CT has become popular for the accurate measurement of craniofacial anatomic structures.[4-8]

The major limitations in previous studies on FA can be summarized as follows: 1) Most studies investigated subjects with skeletal Class I, II, and III malocclusion, causing a problem in sample purity;[9-12] 2) PA cephalograms or facial photographs have inevitable errors in the 2D analysis of a 3D object;[9,11] 3) Although some previous study used 3D-CT analysis, the number of FA patients was insufficient to draw a robust statistical significance;[10] 4) Some previous studies did not provide statistical evidence for the classification of FA;[13-15] 5) Although FA was classified in a 3D manner, most previous studies have focused only on cant and shift. Furthermore, they did not pay attention to the yaw as well as the differences in the frontal ramus angle (FRA) and ramus height (RH);[9-13,15,16] 6) It is important to analyze the asymmetry in the maxilla, maxillary dentition, mandibular dentition, mandible, and mandibular border separately; and 7) Some previous studies failed to consider the clinical significance in relation to pre-operative orthodontic treatment and orthognathic surgery.[12,16]

For clinically significant and statistically valid classification of FA, it is important to conduct studies using 3D-CT images with a large number of patients and full consideration of cant, shift, and yaw. Therefore, the purpose of this study was to classify and characterize the FA phenotypes in Korean adult patients with skeletal Class III malocclusion who had undergone orthognathic surgery using 3D-CT and cluster analysis.

MATERIALS AND METHODS

The initial samples were Korean adult patients who had undergone pre-operative orthodontic treatment and orthognathic surgery at Seoul National University Dental Hospital (SNUDH) in Seoul, Republic of Korea between 2015 and 2020. The inclusion criteria were 1) patients with completed facial growth (over the age of 18 years); 2) patients who were diagnosed with skeletal Class III malocclusion; and 3) patients whose 3D-CT images were taken at least one month prior to orthognathic surgery. The 3D-CTs taken before orthognathic surgery were used to analyze the skeletal problems and set up precise surgical planning and to minimize cost and radiation exposure issues from sequential 3D-CT taken from the initial visit to the post-operative stage. The exclusion criteria were 1) patients whose posterior teeth were missing or abnormally shaped; 2) patients who had a degenerative joint disease, tumor, or trauma history in the temporomandibular joints; and 3) patients who had hemifacial microsomia or other craniofacial anomaly syndromes.

As a result, 120 Korean adult patients who had undergone pre-operative orthodontic treatment and orthognathic surgery for correction of skeletal Class III malocclusion were recruited as the final sample (72 males and 48 females; mean age at the time of 3D-CT taking, 22.9 ± 4.4 years). This study was reviewed and approved by the Institutional Review Board Committee of SNUDH (ERI20029).

3D-CTs (Sensation 10; Siemens, München, Germany; axial slice thickness, 1.0 mm) were taken with centric relation and lips in repose. After each data set was imported into the ON3D program (3DONS, INC., Seoul, Korea), 3D-CT images were re-orientated using the horizontal, coronal, and mid-sagittal planes (Figures 1 and 2, Table 1). The definitions of landmarks and reference planes used in the present study were adopted from the methodology of Hong et al.[17] The N point was registered as the origin (0, 0, 0) of the Cartesian coordinate system.

The definitions of 30 hard tissue landmarks, six lines, and seven planes are enumerated in Figures 1 and 2 and Table 1. These landmarks were identified on each 3D-CT image by a single operator (SWH) with ON3D software.

The definitions of 22 measurement variables are enumerated in Figure 3 and Table 2. In the present study, a novel 3D measurement method was developed to express the cant, shift, and yaw of the maxilla, maxillary dentition, mandibular dentition, mandible, and mandibular border. When asymmetry occurred in the same direction of the Me deviation, the sign of the measurement variables was designated as positive (+); otherwise, the sign was designated as negative (–).

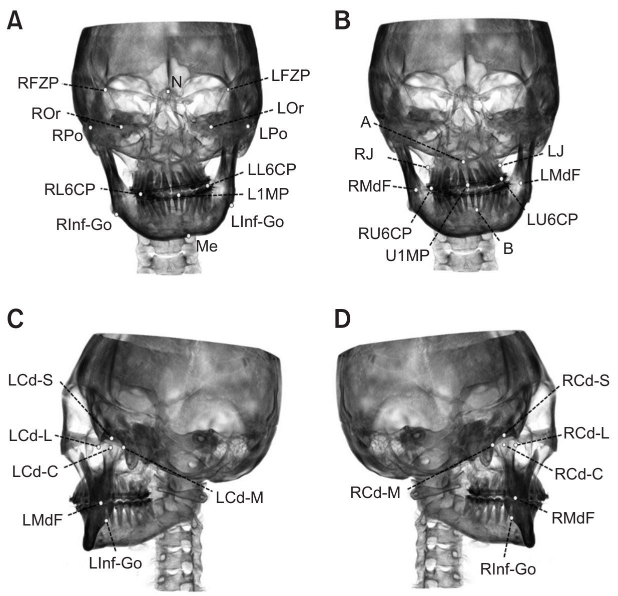

Figure 1. The landmarks used in this study. **A**, Nasion (N), frontozygomatic point, (FZP, R and L), porion (Po, R and L), orbitale (Or, R and L), mesiobuccal (MB) cusp tip of the mandibular first molar (L6CP, R and L), lower dental midline point (L1MP), inferior gonion (Inf-Go, R and L), and menton (Me). **B**, A point (A), jugal process point (J, R and L), mandibular foramen (MdF, R and L), MB cusp tip of the maxillary first molar (U6CP, R and L), B point (B), and upper dental midline point (U1MP). **C** and **D**, Condylion (Cd-S, R and L), lateral pole of condyle (Cd-L, R and L), medial pole of condyle (Cd-M, R and L), and condylar center (Cd-C, R and L).
R, right; L, left.

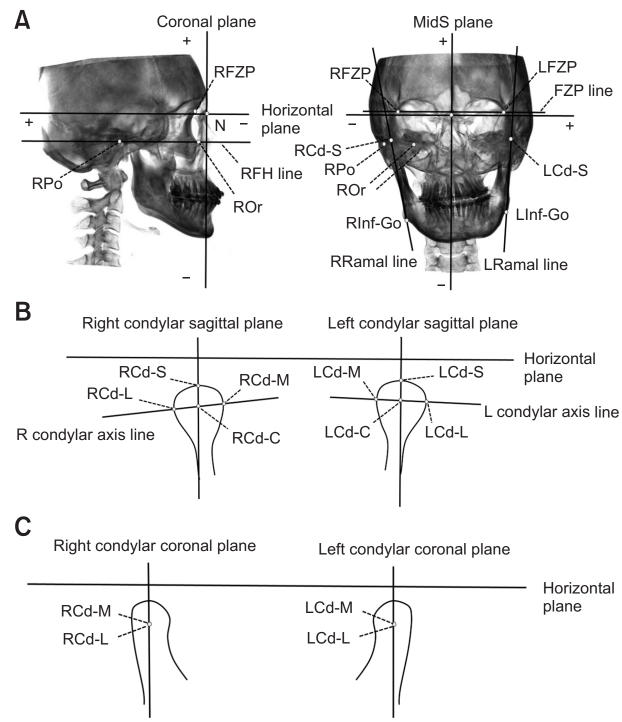

Figure 2. The planes and lines used in this study. **A**, Horizontal plane, coronal plane, mid-sagittal (MidS) plane, frontozygomatic point (FZP) line, right Frankfort horizontal (RFH) line, and ramal line (R and L). **B**, Condylar sagittal plane (R and L) and condylar axis line (R and L). **C**, Condylar coronal plane (R and L).
R, right; L, left.
See Figure 1 for definitions of the other landmarks.

Twelve randomly selected CT images were re-digitized and re-measured after two weeks by the same operator (SWH). Since there was no significant difference in the values of the measurement variables between the first and second measurements in the Wilcoxon signed rank test ($p > 0.05$), the first set of measurements was used for further analysis.

K-means cluster analysis was conducted to classify the FA phenotypes using the three representative variables (cant in the maxillary dentition [molar height difference, mm] and shift [Me deviation, mm] and yaw [°] in the mandibular border), which provide significant clinical information for diagnosis and surgical planning. The reasons were as follows: 1) The cant of the maxillary dentition was used in clustering because it is one of the main targets of orthognathic surgery; and 2) Since the degree of asymmetry worsens from top to bottom, the shift and yaw of the mandibular border were used for clustering. In addition, although we measured both the angle and distance of the cant in the maxillary dentition, only the cant distance (molar height difference) was utilized for clustering to prevent overfitting and to provide clinical information for easy application in surgical planning.

According to the total within-cluster sum of squares, the appropriate number of clusters was 4 to 6. After analyzing the results of clustering by the number of clusters with a 3D scatter plot, the final number of clusters was determined to be five.

Among the five clusters, the cluster with the least amounts of shift, cant, and yaw was designated as the non-asymmetry type (Table 3). The degree of asymmetry in each measurement variable was classified into normal, mild, moderate, and severe based on the means and standard deviations (SD) of the non-asymmetry type (Table 3). The cut-points were 1 SD to 2 SD or –1 SD to –2 SD for mild degree, 2 SD to 3 SD or –2 SD to –3 SD for moderate degree, and > 3 SD or < –3 SD for severe degree. The one-way analysis of variance test and multiple comparisons with Tukey's honestly significant difference test were conducted to characterize the differences in the FA variables among the five clusters.

 https://doi.org/10.4041/kjod.2022.52.2.85

Table 1. Definition of the landmarks, lines, and planes used in this study

Landmarks, lines and planes	Abbreviation	Definition
Cranial landmarks		
Nasion	N	The middle point of nasofrontal suture
Right frontozygomatic suture	RFZP	The intersection of the right frontozygomatic suture and the inner rim of the orbit
Left frontozygomatic suture	LFZP	The intersection of the left frontozygomatic suture and the inner rim of the orbit
Right porion	RPo	The most superior point of the right external auditory meatus
Left porion	LPo	The most superior point of the left external auditory meatus
Maxillary skeletal landmarks		
Right orbitale	ROr	The most inferior point of the right orbital contour
Left orbitale	LOr	The most inferior point of the left orbital contour
Right jugal process point	RJ	The intersection point between the lateral contour of the alveolar process and the lower contour of the zygomatic buttress of the right maxilla
Left jugal process point	LJ	The intersection point of the lateral contour of the alveolar process and the lower contour of the zygomatic buttress of the left maxilla
A point	A	The deepest point between the anterior nasal spine and the upper incisal alveolus in the mid-sagittal plane
Maxillary dental landmarks		
Maxillary central incisor	U1MP	Upper dental midline point
Cusp of the maxillary right first molar	RU6CP	The tip of the mesiobuccal cusp of the maxillary right first molar crown
Cusp of the maxillary left first molar	LU6CP	The tip of the mesiobuccal cusp of the maxillary left first molar crown
Mandibular skeletal landmarks		
Right mandibular foramen	RMdF	The most Inferior point of the right mandibular foramen
Left mandibular foramen	LMdF	The most inferior point of the left mandibular foramen
B point	B	The deepest point between pogonion and the lower incisal alveolus in the mid-sagittal plane
Menton	Me	The most inferior point in the middle of the mandibular chin in the coronal plane
Right condylion	RCd-S	The most superior point of the right condyle in the condylar sagittal plane within the range of glenoid fossa
Left condylion	LCd-S	The most superior point of the left condyle in the condylar sagittal plane within the range of glenoid fossa
Lateral pole of the right condyle	RCd-L	The most lateral point of the right condylar head
Lateral pole of the left condyle	LCd-L	The most lateral point of the left condylar head
Medial pole of the right condyle	RCd-M	The most medial point of the right condylar head
Medial pole of the left condyle	LCd-M	The most medial point of the left condylar head
Right condylar center	RCd-C	A mid-point between the RCd-L and RCd-M
Leftt condylar center	LCd-C	A mid-point between the LCd-L and LCd-M
Right inferior gonion	RInf-Go	The most inferior point of the inferior border of the lower half of the right ramus
Left inferior gonion	LInf-Go	The most inferior point of the inferior border of the lower half of the left ramus

Table 1. Continued

Landmarks, lines and planes	Abbreviation	Definition
Mandibular dental landmarks		
Mandibular central incisor	L1MP	Lower dental midline point
Cusp of mandibular right first molar	RL6CP	The mesiobuccal cusp tip of the mandibular right first molar
Cusp of mandibular left first molar	LL6CP	The mesiobuccal cusp tip of the mandibular left first molar
Lines		
Frontozygomatic point line	FZP line	A line passing through the RFZP and LFZP
Right Frankfort horizontal line	RFH line	A line passing through the RPo and ROr
Right ramal line	RRamal line	A line passing through the RInf Go and RCd-S
Left ramal line	LRamal line	A line passing through the LInf Go and LCd-S
Right condylar axis line	RCondylar axis line	A line passing through the RCd-L and RCd-M
Left condylar axis line	LCondylar axis line	A line passing through the LCd-L and LCd-M
Planes		
Horizontal plane	Horizontal plane	A plane parallel to both the RFH line and the FZP line passing N
Coronal plane	Coronal plane	A plane perpendicular to both the horizontal plane and the FZP line passing through N
Mid-sagittal plane	MidS plane	A plane perpendicular to both the horizontal plane and the coronal plane passing through N
Right condylar coronal plane	RCondylar coronal plane	A plane including the RCondylar axis line and perpendicular to the horizontal plane
Left condylar coronal plane	LCondylar coronal plane	A plane including the LCondylar axis line and perpendicular to the horizontal plane
Right condylar sagittal plane	RCondylar sagittal plane	A plane including the RCd-C point and perpendicular to the horizontal plane and the RCondylar coronal plane
Left condylar sagittal plane	LCondylar sagittal plane	A plane including the LCd-C point and perpendicular to the horizontal plane and the LCondylar coronal plane

Adapted from the article of Hong et al. (Korean J Orthod 2020;50:293-303).[17]

All statistical analyses were conducted using Language R, version 3.6.3 (The R Foundation for Statistical Computing, Vienna, Austria). p-value less than 0.05 was considered statistically significant.

RESULTS

Morphological characteristics of five FA phenotypes (Table 4, Figure 4)

The FA phenotypes in Class III patients were classified into five types according to their distinct morphological characteristics: non-asymmetry type (n = 43, 35.8%), maxillary-cant (Max-Cant) type (n = 17, 14.2%), mandibular-shift and yaw (Man-Shift-Yaw) type (n = 20, 16.7%), complex type (n = 11, 9.2%), and maxillary reverse-cant (Max-Rev-Cant) type (n = 29, 24.2%). In the non-asymmetry type, no significant asymmetry was observed.

The Max-Cant type demonstrated severe cant in the maxillary dentition (MxD-Cant, 2.9°, 2.7 mm) and mild cant in the mandibular dentition (MdD-Cant, 2.4°, 2.0 mm). A mild shift was observed in the mandible and mandibular border (MdS-Shift, 3.1 mm; MdB-Shift, 4.1 mm).

The Man-Shift-Yaw type exhibited moderate shift and mild yaw in the mandibular dentition (MdD-Shift, 4.7 mm; MdD-Yaw, 3.7°), moderate shift and yaw in the mandible (MdS-Shift, 5.4 mm; MdS-Yaw, 4.1°) and the mandibular border (MdB-Shift, 6.5 mm; MdB-Yaw, 4.5°), and mild RH-difference (3.4 mm). In addition, a mild cant was observed in the mandibular dentition (MdD-Cant, 2.2°, 1.8 mm).

The complex type demonstrated severe cant in the maxillary dentition (MxD-Cant, 3.4°, 3.2 mm); severe

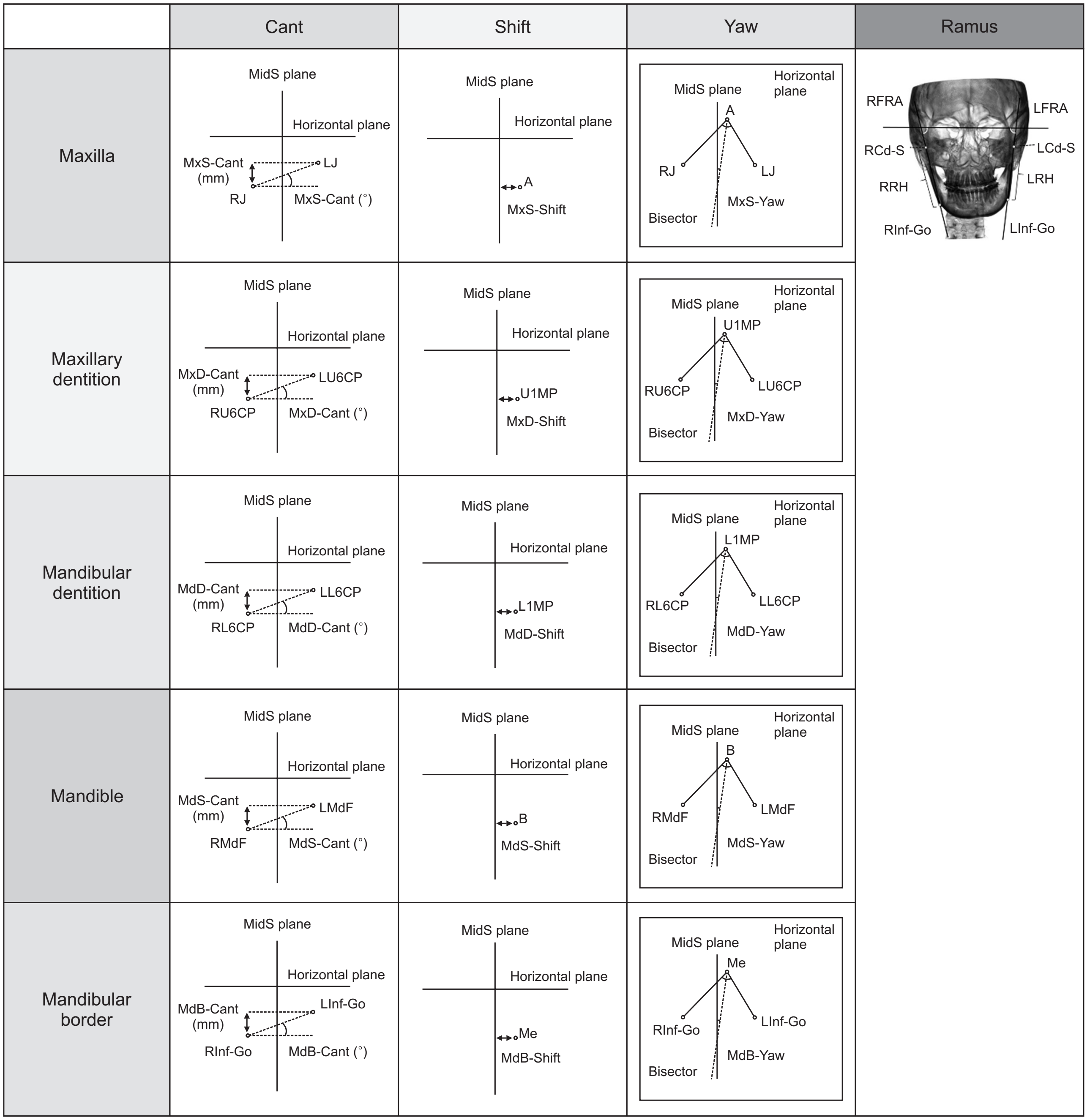

Figure 3. The variables used in this study. Maxillary skeletal (MxS)-Cant (°), MxS-Cant (mm), MxS-Shift (mm), MxS-Yaw (°), maxillary dental (MxD)-Cant (°), MxD-Cant (mm), MxD-Shift (mm), MxD-Yaw (°), mandibular dental (MdD)-Cant (°), MdD-Cant (mm), MdD-Shift (mm), MdD-Yaw (°), mandibular skeletal (MdS)-Cant (°), MdS-Cant (mm), MdS-Shift (mm), MdS-Yaw (°), mandibular border (MdB)-Cant (°), MdB-Cant (mm), MdB-Shift (mm), MdB-Yaw (°), frontal ramus angle (FRA, °) (R and L, difference), Ramus height (RH, mm) (R and L, difference).
MidS, mid-sagittal; R, right; L, left.
See Figure 1 for definitions of the other landmarks.

shift and yaw in the mandibular dentition (MdD-Shift, 8.7 mm; MdD-Yaw, 7.0°), mandible (MdD-Shift, 10.3 mm; MdD-Yaw, 7.1°), and mandibular border (MdB-Shift, 13.7 mm; MdB-Yaw, 8.5°); and moderate FRA-difference (7.3°) and RH-difference (8.4 mm). Mild cant in the maxilla (MxS-Cant, 2.1°, 2.1 mm), severe cant in

Table 2. Definition of the variables used in this study

		Variable	Abbreviation	Definition
Cant	Angulation	Maxillary skeletal Cant (°)	MxS-Cant (°)	The angle formed between the RJ–LJ line and the FZP line projected to the Coronal plane
		Maxillary dental Cant (°)	MxD-Cant (°)	The angle formed between the RU6CP–LU6CP line and the FZP line projected to the Coronal plane
		Mandibular dental Cant (°)	MdD-Cant (°)	The angle formed between the RL6CP–LL6CP line and the FZP line projected to the Coronal plane
		Mandibular skeletal Cant (°)	MdS-Cant (°)	The angle formed between the RMdF–LMdF line and the FZP line projected to the Coronal plane
		Mandibular border Cant (°)	MdB-Cant (°)	The angle formed between the RInf-Go–LInf-Go line and the FZP line projected to the Coronal plane
	Distance	Maxillary skeletal Cant (mm)	MxS-Cant (mm)	The difference in the coordinates on the z-axis of RJ and LJ
		Maxillary dental Cant (mm)	MxD-Cant (mm)	The difference in the coordinates on the z-axis of RU6CP and LU6CP
		Mandibular dental Cant (mm)	MdD-Cant (mm)	The difference in the coordinates on the z-axis of RL6CP and LL6CP
		Mandibular skeletal Cant (mm)	MdS-Cant (mm)	The difference in the coordinates on the z-axis of RMdF and LMdF
		Mandibular border Cant (mm)	MdB-Cant (mm)	The difference in the coordinates on the z-axis of RInf-Go and LInf-Go
Shift		Maxillary skeletal Shift (mm)	MxS-Shift (mm)	The x-axis coordinate of A point
		Maxillary dental Shift (mm)	MxD-Shift (mm)	The x-axis coordinate of U1MP
		Mandibular dental Shift (mm)	MdD-Shift (mm)	The x-axis coordinate of L1MP
		Mandibular skeletal Shift (mm)	MdS-Shift (mm)	The x-axis coordinate of B point
		Mandibular border Shift (mm)	MdB-Shift (mm)	The x-axis coordinate of Me
Yaw		Maxillary skeletal Yaw (°)	MxS-Yaw (°)	The angle between the bisector of the RJ–A–LJ angle and the MidS plane projected to the Horizontal plane
		Maxillary dental Yaw (°)	MxD-Yaw (°)	The angle between the bisector of the RU6CP–U1MP–LU6CP angle and the MidS plane projected to the Horizontal plane
		Mandibular dental Yaw (°)	MdD-Yaw (°)	The angle between the bisector of the RL6CP–L1MP–LL6CP angle and the MidS plane projected to the Horizontal plane
		Mandibular skeletal Yaw (°)	MdS-Yaw (°)	The angle between the bisector of the RMdF–B–LMdF angle and the MidS plane projected to the Horizontal plane
		Mandibular border Yaw (°)	MdB-Yaw (°)	The angle between the bisector of the RInf-Go–Me–LInf-Go angle and the MidS plane projected to the Horizontal plane
Ramus		Frontal ramus angle difference between the right and left sides (°)	FRA-difference (°)	The difference between the RFRA (the angle formed between RRamal line and the FZP line projected to the Coronal plane) and the LFRA (the angle formed between the LRamal line and the FZP line projected to the Coronal plane)
		Ramus height difference between the right and left sides (mm)	RH-difference (mm)	The difference between the RRH (the linear distance from RInf-Go to RCd-S) and the LRH (the linear distance from LInf-Go to LCd-S)

See Table 1 for definitions of each landmark, line, and plane.

 https://doi.org/10.4041/kjod.2022.52.2.85

Table 3. Severity of the measurement variables

	Variable	Severe (< −3 SD)	Moderate (≥ −3 SD and < −2 SD)	Mild (≥ −2 SD and < −1 SD)	Normal (≥ −1 SD and ≤ 1 SD)	Mild (> 1 SD and ≤ 2 SD)	Moderate (> 2 SD and ≤ 3 SD)	Severe (> 3 SD)
Cant	MxS-Cant (°)	< −3.30	≥ −3.30 and < −2.06	≥ −2.06 and < −0.82	≥ −0.82 and ≤ 1.65	> 1.65 and ≤ 2.89	> 2.89 and ≤ 4.13	> 4.13
	MxD-Cant (°)	< −0.69	≥ −0.69 and < −0.18	≥ −0.18 and < 0.32	≥ 0.32 and ≤ 1.33	> 1.33 and ≤ 1.84	> 1.84 and ≤ 2.34	> 2.34
	MdD-Cant (°)	< −2.07	≥ −2.07 and < −1.11	≥ −1.11 and < −0.16	≥ −0.16 and ≤ 1.75	> 1.75 and ≤ 2.71	> 2.71 and ≤ 3.67	> 3.67
	MdS-Cant (°)	< −2.72	≥ −2.72 and < −1.61	≥ −1.61 and < −0.50	≥ −0.50 and ≤ 1.72	> 1.72 and ≤ 2.82	> 2.82 and ≤ 3.93	> 3.93
	MdB-Cant (°)	< −3.92	≥ −3.92 and < −2.44	≥ −2.44 and < −0.96	≥ −0.96 and ≤ 2.00	> 2.00 and ≤ 3.48	> 3.48 and ≤ 4.96	> 4.96
	MxS-Cant (mm)	< −3.50	≥ −3.50 and < −2.18	≥ −2.18 and < −0.87	≥ −0.87 and ≤ 1.76	> 1.76 and ≤ 3.08	> 3.08 and ≤ 4.40	> 4.40
	MxD-Cant (mm)	< −0.60	≥ −0.60 and < −0.15	≥ −0.15 and < 0.30	≥ 0.30 and ≤ 1.20	> 1.20 and ≤ 1.65	> 1.65 and ≤ 2.10	> 2.10
	MdD-Cant (mm)	< −1.72	≥ −1.72 and < −0.92	≥ −0.92 and < −0.13	≥ −0.13 and ≤ 1.46	> 1.46 and ≤ 2.26	> 2.26 and ≤ 3.05	> 3.05
	MdS-Cant (mm)	< −4.03	≥ −4.03 and < −2.39	≥ −2.39 and < −0.74	≥ −0.74 and ≤ 2.54	> 2.54 and ≤ 4.19	> 4.19 and ≤ 5.83	> 5.83
	MdB-Cant (mm)	< −6.36	≥ −6.36 and < −3.96	≥ −3.96 and < −1.55	≥ −1.55 and ≤ 3.25	> 3.25 and ≤ 5.65	> 5.65 and ≤ 8.05	> 8.05
Shift	MxS-Shift (mm)	< −3.14	≥ −3.14 and < −2.01	≥ −2.01 and < −0.87	≥ −0.87 and ≤ 1.39	> 1.39 and ≤ 2.52	> 2.52 and ≤ 3.66	> 3.66
	MxD-Shift (mm)	< −4.07	≥ −4.07 and < −2.56	≥ −2.56 and < −1.05	≥ −1.05 and ≤ 1.96	> 1.96 and ≤ 3.46	> 3.46 and ≤ 4.97	> 4.97
	MdD-Shift (mm)	< −3.01	≥ −3.01 and < −1.50	≥ −1.50 and < 0.02	≥ 0.02 and ≤ 3.06	> 3.06 and ≤ 4.58	> 4.58 and ≤ 6.10	> 6.10
	MdS-Shift (mm)	< −3.08	≥ −3.08 and < −1.53	≥ −1.53 and < 0.03	≥ 0.03 and ≤ 3.13	> 3.13 and ≤ 4.69	> 4.69 and ≤ 6.24	> 6.24
	MdB-Shift (mm)	< −2.21	≥ −2.21 and < −0.74	≥ −0.74 and < 0.73	≥ 0.73 and ≤ 3.67	> 3.67 and ≤ 5.14	> 5.14 and ≤ 6.61	> 6.61
Yaw	MxS-Yaw (°)	< −4.84	≥ −4.84 and < −3.27	≥ −3.27 and < −1.71	≥ −1.71 and ≤ 1.43	> 1.43 and ≤ 3.00	> 3.00 and ≤ 4.56	> 4.56
	MxD-Yaw (°)	< −6.16	≥ −6.16 and < −4.29	≥ −4.29 and < −2.42	≥ −2.42 and ≤ 1.32	> 1.32 and ≤ 3.19	> 3.19 and ≤ 5.06	> 5.06
	MdD-Yaw (°)	< −5.39	≥ −5.39 and < −3.46	≥ −3.46 and < −1.52	≥ −1.52 and ≤ 2.34	> 2.34 and ≤ 4.27	> 4.27 and ≤ 6.21	> 6.21
	MdS-Yaw (°)	< −4.17	≥ −4.17 and < −2.66	≥ −2.66 and < −1.15	≥ −1.15 and ≤ 1.87	> 1.87 and ≤ 3.39	> 3.39 and ≤ 4.90	> 4.90
	MdB-Yaw (°)	< −3.76	≥ −3.76 and < −2.33	≥ −2.33 and < −0.90	≥ −0.90 and ≤ 1.97	> 1.97 and ≤ 3.40	> 3.40 and ≤ 4.83	> 4.83
Ramus	FRA-difference (°)	< −5.65	≥ −5.65 and < −3.21	≥ −3.21 and < −0.77	≥ −0.77 and ≤ 4.10	> 4.10 and ≤ 6.53	> 6.53 and ≤ 8.97	> 8.97
	RH-difference (mm)	< −7.25	≥ −7.25 and < −4.62	≥ −4.62 and < −1.98	≥ −1.98 and ≤ 3.29	> 3.29 and ≤ 5.92	> 5.92 and ≤ 8.56	> 8.56

The mean and standard deviation (SD) from the non-asymmetry group were used for deciding the severity of each variable.
See Table 2 for definitions of each measurement variable.

Table 4. Comparison of measurement variables among the facial asymmetry types

Parameter			Non-asymmetry type (n = 43, 35.8%, 1)		Max-Cant type (n = 17, 14.2%, 2)		Man-Shift-Yaw type (n = 20, 16.7%, 3)		Complex type (n = 11, 9.2%, 4)		Max-Rev-Cant type (n = 29, 24.2%, 5)		*p*-value	Multiple comparison
			Mean	SD	Mean	SD	Mean	SD	Mean	SD	Mean	SD		
Cant	Angulation	MxS-Cant (°)	0.41	1.24	1.15	1.11	1.04	2.24	$2.05^{\dagger}$	1.54	−0.80	1.17	< 0.001***	5 < (1, 3, 2) < (3, 2, 4)
		MxD-Cant (°)	0.83	0.50	2.87^{c}	0.96	1.03	0.85	3.40^{c}	1.67	-0.87^{c}	0.61	< 0.001***	5 < (1, 3) < (2, 4)
		MdD-Cant (°)	0.80	0.96	$2.35^{\dagger}$	1.05	$2.15^{\dagger}$	1.56	5.44^{c}	1.46	0.01	1.13	< 0.001***	(5, 1) < (3, 2) < 4
		MdS-Cant (°)	0.61	1.11	1.05	0.91	1.30	1.58	3.81^{b}	1.46	−0.30	1.74	< 0.001***	(5, 1) < (1, 2, 3) < 4
		MdB-Cant (°)	0.52	1.48	1.17	0.98	1.36	1.60	3.94^{b}	1.80	0.17	1.73	< 0.001***	(5, 1, 2, 3) < 4
		p-value	0.363		< 0.001***		0.207		< 0.001***		< 0.011*			
		Multiple comparison			(MdS, MxS, MdB) < (MdD, MxD)				(MxS, MxD, MdS, MdB) < (MdS, MdB, MdD)		(MxD, MxS, MdS, MdD) < (MxS, MdS, MdD, MdB)			
	Distance	MxS-Cant (mm)	0.45	1.32	1.26	1.22	1.07	2.22	$2.13^{\dagger}$	1.51	−0.84	1.22	< 0.001***	5 < (1, 3, 2) < (3, 2, 4)
		MxD-Cant (mm)	0.75	0.45	$2.69^{\S}$	0.91	0.94	0.79	$3.20^{\S}$	1.56	$-0.81^{\S}$	0.58	< 0.001***	5 < (1, 3) < (2, 4)
		MdD-Cant (mm)	0.67	0.79	$2.01^{\dagger}$	0.89	$1.82^{\dagger}$	1.34	$4.65^{\S}$	1.35	0.02	0.93	< 0.001***	(5, 1) < (3, 2) < 4
		MdS-Cant (mm)	0.90	1.64	1.63	1.39	2.00	2.36	$5.74^{\ddagger}$	2.12	−0.42	2.54	< 0.001***	(5, 1) < (1, 2, 3) < 4
		MdB-Cant (mm)	0.85	2.40	1.92	1.67	2.17	2.57	$6.39^{\ddagger}$	2.95	0.27	2.83	< 0.001***	(5, 1, 2, 3) < 4
		p-value	0.664		< 0.028*		0.204		< 0.001***		< 0.096			
		Multiple comparison			(MxS, MdS, MdB, MdD) < (MdS, MdB, MdD, MxD)				(MxS, MxD) < (MxD, MdD) < (MdD, MdS, MdB)					
Shift		MxS-Shift (mm)	0.26	1.13	−0.23	1.86	0.69	1.30	0.88	1.17	0.48	0.79	0.122	
		MxD-Shift (mm)	0.45	1.51	0.91	2.10	1.37	1.28	1.92	1.52	0.49	1.45	0.029*	
		MdD-Shift (mm)	1.54	1.52	2.53	2.17	$4.68^{\ddagger}$	1.58	$8.65^{\S}$	1.74	1.83	1.68	< 0.001***	(1, 5, 2) < 3 < 4
		MdS-Shift (mm)	1.58	1.55	$3.14^{\dagger}$	2.13	$5.39^{\ddagger}$	1.47	$10.25^{\S}$	2.11	1.82	1.49	< 0.001***	(1, 5) < (5, 2) < 3 < 4
		MdB-Shift (mm)	2.20	1.47	$4.05^{\dagger}$	2.07	$6.51^{\ddagger}$	1.58	$13.73^{\S}$	2.79	2.19	1.49	< 0.001***	(5, 1) < 2 < 3 < 4
		p-value	< 0.001***		< 0.001***		< 0.001***		< 0.001***		< 0.001***			
		Multiple comparison	(MxS, MxD) < (MdD, MdS, MdB)		(MxS, MxD) < (MxD, MdD) < (MdD, MdS, MdB)		(MxS, MxD) < (MdD, MdS) < (MdS, MdB)		(MxS, MxD) < (MdD, MdS) < MdB		(MxD, MxS, MdS, MdD) < (MxS, MdS, MdD, MdB)			
Yaw		MxS-Yaw (°)	−0.14	1.57	−0.03	1.81	0.64	1.49	1.19	1.37	−0.24	1.35	0.042*	
		MxD-Yaw (°)	−0.55	1.87	−0.12	1.60	0.18	2.00	−0.14	1.20	−0.32	1.92	0.677	
		MdD-Yaw (°)	0.41	1.93	1.42	1.74	$3.72^{\dagger}$	1.63	$6.97^{\S}$	2.29	1.03	1.85	< 0.001***	(1, 5, 2) < 3 < 4
		MdS-Yaw (°)	0.36	1.51	1.62	1.47	$4.05^{\ddagger}$	1.40	$7.13^{\S}$	2.29	1.08	1.09	< 0.001***	(1, 5) < (5, 2) < 3 < 4
		MdB-Yaw (°)	0.53	1.43	1.73	1.29	$4.52^{\ddagger}$	1.42	$8.54^{\S}$	2.37	1.36	1.32	< 0.001***	(5, 1, 2) < 3 < 4
		p-value	0.017*		< 0.001***		< 0.001***		< 0.001***		< 0.001***			
		Multiple comparison	(MxD, MxS, MdS, MdD) < (MxS, MdS, MdD, MdB)		(MxD, MxS, MdD) < (MdD, MdS, MdB)		(MxD, MxS) < (MdD, MdS, MdB)		(MxD, MxS) < (MdD, MdS, MdB)		(MxD, MxS) < (MdD, MdS, MdB)			

https://doi.org/10.4041/kjod.2022.52.2.85

Table 4. Continued

Parameter		Non-asymmetry type (n = 43, 35.8%, 1)		Max-Cant type (n = 17, 14.2%, 2)		Man-Shift-Yaw type (n = 20, 16.7%, 3)		Complex type (n = 11, 9.2%, 4)		Max-Rev-Cant type (n = 29, 24.2%, 5)		*p*-value	Multiple comparison
		Mean	SD	Mean	SD	Mean	SD	Mean	SD	Mean	SD		
Ramus	FRA-difference (°)	1.66	2.44	2.25	2.54	2.74	2.01	7.33‡	2.54	1.35	2.27	< 0.001***	(5, 1, 2, 3) < 4
	RH-difference (mm)	0.65	2.63	2.08	2.26	3.42†	2.46	8.41‡	3.06	0.24	2.87	< 0.001***	(5, 1, 2) < (2, 3) < 4

The K-mean cluster analysis was conducted using three representative variables, which provide significant clinical information: MxD-Cant (mm), MdB-Shift (mm), and MdB-Yaw (°).
The one-way analysis of variance test with Tukey's honestly significant difference *post hoc* comparison was conducted.
**p* < 0.05; ****p* < 0.001.
†Mild; ‡Moderate; §Severe.
See Table 2 for definitions of each measurement variable.

the mandibular dentition (MdD-Cant, 5.4°, 4.7 mm), and moderate cant in the mandible (MdS-Cant, 3.8°, 5.7 mm) and mandibular border (MdB-Cant, 3.9°, 6.4 mm) were also observed.

The Max-Rev-Cant type revealed that the cant in the maxillary dentition (MxD-Cant, −0.9°, −0.8 mm) was expressed into the opposite direction of the Me deviation. However, there was no significant asymmetry in the mandibular border (MdB-Cant, 0.2°, 0.3 mm; MdB-Shift, 2.2 mm; MdB-Yaw, 1.4°).

Comparison of cant, yaw, and shift among the FA phenotypes (Table 4, Figure 4)

Cant was most significant in all parts in the complex type (MxS-Cant, 2.1°, 2.1 mm; MxD-Cant, 3.4°, 3.2 mm; MdD-Cant, 5.4°, 4.7 mm; MdS-Cant, 3.8°, 5.7 mm; MdB-Cant, 3.9°, 6.4 mm); followed by the maxillary and mandibular dentition in the Max-Cant type (MxD-Cant, 2.9°, 2.7 mm; MdD-Cant, 2.4°, 2.0 mm); and the mandibular dentition in the Man-Shift-Yaw type (MdD-Cant 2.2°, 1.8 mm) (all $p < 0.001$). However, in the Max-Rev-Cant type, reverse cant was observed at the maxilla and maxillary dentition (−0.8°, −0.8 mm and −0.9°, −0.8 mm; all $p < 0.001$).

Shift was most significant in the mandibular dentition, mandible, and mandibular border of the complex type (MdD-Shift, 8.7 mm; MdS-Shift, 10.3 mm; MdB-Shift, 13.7 mm); followed by the Man-Shift-Yaw type (MdD-Shift, 4.7 mm; MdS-Shift, 5.4 mm; MdB-Shift, 6.5 mm); and the mandible and mandibular border of the Max-Cant type (MdS-Shift, 3.1 mm; MdB-Shift, 4.1 mm) (all $p < 0.001$).

Yaw was most significant in the mandibular dentition, mandible, and mandibular border of the complex type, followed by the Man-Shift-Yaw type (MdD-Yaw, 7.0°, 3.7°; MdS-Yaw, 7.1°, 4.1°; MdB-Yaw, 8.5°, 4.5°; all $p < 0.001$).

DISCUSSION

Classification of the FA phenotypes (Tables 4 and 5, Figure 5)

Approximately two-thirds (64.2%) of Class III patients who underwent orthognathic surgery had a significant FA. They were divided into four major FA clusters according to the existence of the shift and yaw in the mandibular border, the cant in the maxillary dentition, and a combination of these asymmetries (Man-Shift-Yaw type, Max-Cant type, Max-Rev-Cant type, and complex type; Figure 6). This finding was somewhat different from the classification of previous cluster analysis studies[9,10,18] and a non-cluster analysis study (Table 5).[15]

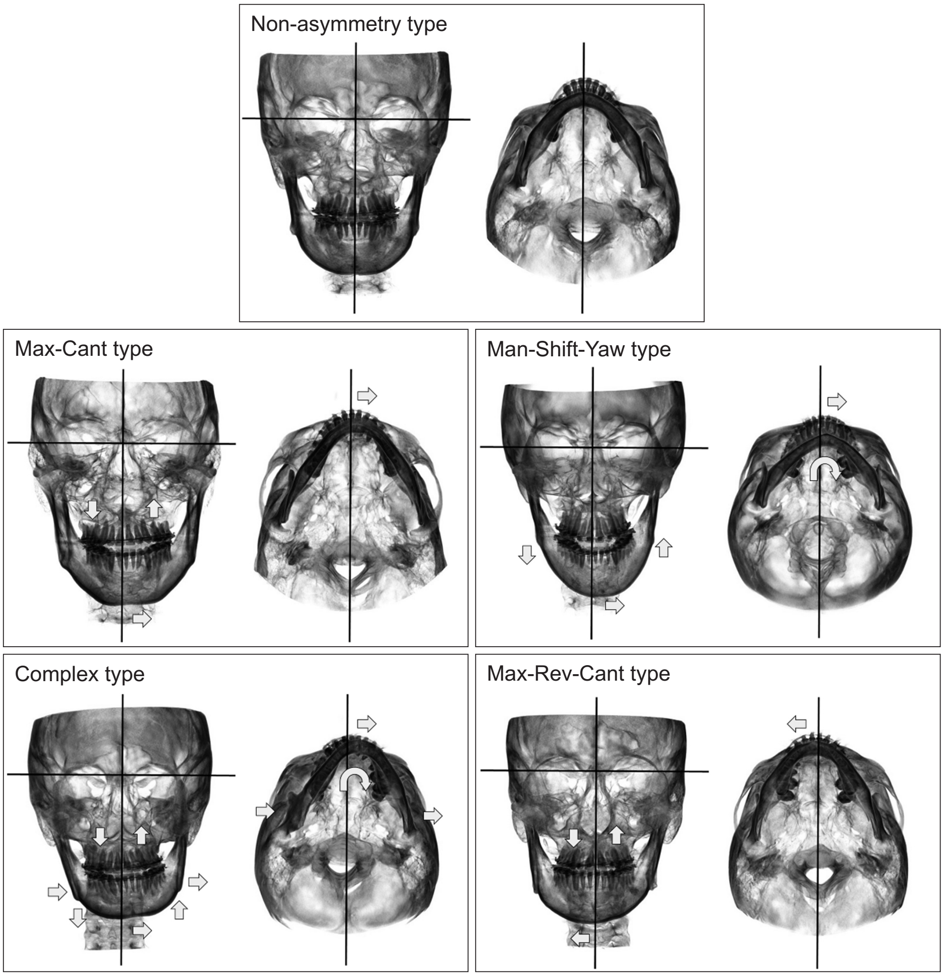

Figure 4. Examples of the non-asymmetry type and 4 facial asymmetry phenotypes. 1) Non-asymmetry type (35.8%); 2) maxillary-cant (Max-Cant) type (14.2%; severe cant of the maxillary dentition, mild shift of the mandibular border); 3) mandibular-shift and yaw (Man-Shift-Yaw) type (16.7%; moderate shift and yaw of the mandibular border, mild ramus height difference); 4) complex type (9.2%; severe cant of the maxillary dentition, moderate cant, severe shift, and severe yaw of the mandibular border, moderate differences in frontal ramus angle and ramus height); and 5) maxillary reverse-cant (Max-Rev-Cant) type (24.2%; reverse-cant of the maxillary dentition).

Characteristics of each FA phenotype (Tables 4 and 5, Figure 5)

The Max-Cant type was characterized by severe cant and molar height differences in the maxillary dentition, and mild cant and molar height differences in the mandibular dentition. These values indicated the remaining amounts of transverse occlusal plane (OP) cant and molar height difference after vertical decompensation by pre-operative orthodontic treatment. In addition, a mild shift of the mandibular border (Me deviation) into the deviated side, which might be induced by the cant of the maxilla. Since there was no significant difference in RH, the FA of the Max-Cant type in this study might not be caused by unilateral condylar hyperplasia.

The Man-Shift-Yaw type was characterized by moderate shift and yaw in the mandibular border and mild RH-difference. When the shift of the mandible occurs in the deviated side, it usually exhibits different molar inclinations (transverse buccolingual compensation). When the yaw of the mandible occurs in the deviated side, it results in an asymmetric molar relationship, distorted dental arch form, and discrepancy between the dental and basal arches (horizontal compensation). Moreover, the Man-Shift-Yaw type exhibited a mild cant and molar height difference in the mandibular. Since there was no significant cant in the maxillary dentition, the cant and molar height difference in the mandibular dentition might occur due to the shift and yaw of the mandible. Joondeph[19] suggested that a functional shift at an early age might lead to remodeling of the condyle and glenoid fossa, resulting in asymmetric growth of the mandible.

Since the complex type was characterized by a combination of the Max-Cant type and the Man-Shift-Yaw type, it showed more complicated features of vertical, transverse, and horizontal dentoalveolar compensation. Since patients with hemifacial microsomia and other craniofacial anomalies were excluded in this study, the asymmetric growth of the mandible and compensation of the maxilla might be the causes of this FA type rather than a problem of the cranial base, at least in Class III patients.

In the Max-Rev-Cant type, since there was no significant asymmetry in the mandibular border, the reverse

 https://doi.org/10.4041/kjod.2022.52.2.85

Table 5. Comparison of facial asymmetry classifications between this and previous studies

Phenotype	This study	Hwang et al.[9] Hwang et al.[18]	Baek et al.[10]	Chen et al.[15]
Samples				
Ethnicity	Korean	Korean	Korean	Taiwanese
Subjects	Patients who underwent orthognathic surgery	Patients who were diagnosed with facial asymmetry	Patients who wanted correction of facial asymmetry	Patients who wanted correction of facial asymmetry
Number	120	100	43	70
Study design				
Angle classification	Skeletal Class III	Skeletal Class I, II, and III	Skeletal Class I, II, and III	Skeletal Class III
Exclusion criteria	• Posterior teeth were missing or abnormally shaped • Degenerative joint disease, tumor, or trauma history in the temporomandibular joints • Hemifacial microsomia and other craniofacial syndromes	• Not mentioned	• Cleft lip and/or palate, plagiocephaly, hemifacial microsomia • Congenital muscular torticollis • Degenerative temporomandibular joint disease • Mandibular tumors • History of trauma to the jaw	• Congenital anomalies • History of maxillofacial trauma
Reference planes	Horizontal plane Coronal plane Mid-sagittal plane	Frankfort horizontal plane Mid-sagittal reference line	Frankfort horizontal plane Coronal plane Mid-sagittal plane	Mid-sagittal plane Horizontal plane Coronal plane
Origin (0, 0, 0)	N point	None	Not mentioned	Not mentioned
Variables for classification	Max-dental Cant (mm) Man-border Shift (mm) Man-border Yaw (°)	Menton deviation (°) Apical base midline discrepancy (mm) Vertical difference of the right and left Ag (mm) Horizontal difference of the right and left Ag (mm) Maxillary base canting (°) Maxillary alveolar canting (°) Bulkiness difference of the mandibular inferior border Lip line canting (°)	Upper midline deviation (mm) Maxilla canting of U3 and U6 (mm) Arch form discrepancy (mm) Gonion to the mid-sagittal plane (mm) Ramus height (mm) Frontal ramus inclination (°) Menton deviation (mm)	The direction and magnitude of transverse ramus discrepancy relative to menton deviation
Inclusion of yaw	Yes	No	No	No
Analyzed data	3D-CT	PA cephalogram and frontal photograph	3D-CT	CBCT
Statistical method	Cluster analysis	Cluster analysis	Cluster analysis	No cluster

Table 5. Continued

Phenotype	This study	Hwang et al.[9] Hwang et al.[18]	Baek et al.[10]	Chen et al.[15]
Types	Non-asymmetry type (35.8%)	Group E (Normal, 28%) • All variables were within normal limits	Not mentioned	Not mentioned
	Max-Cant type (14.2%)	Not mentioned	Group 2 (Universal lateral condylar hyperplasia asymmetry, 39%) • Significant difference between the left and right ramus height • Menton deviation to the short side	Not mentioned
	Man-Shift-Yaw type (16.7%)	Group C (Menton type, 21%) • No ramus height difference between the deviated and non-deviated sides • Deviation of menton and lower apical base midline to the same side	Group 1 (Mandibular body asymmetry, 44%) • Shift or lateralization of the mandibular body	Group 2 (27%) • Menton and ramus deviation to the same side • Discrepancy in the ramus width was larger than the menton shift • Asymmetry resulted from a bodily side shift of the maxillomandibular complex without significant cant and yaw
	Complex type (9.2%)	Group A (Ramus–Menton type, 7%) • Significant canting of the maxillary basal and alveolar bone • Deviation of menton and mandibular apical base midline to the side of the shorter ramus • Difference of the right and left ramus height	Group 4 (C-shaped asymmetry, 5%) • Severe maxillary canting • Significant ramus height differences • Significant menton deviation to the short side	Group 1 (47%) • Large shift of menton • Synchronous but smaller ramus deviation • The maxillomandibular complex had cant and yaw to the menton deviation side • Maxillary and dental asymmetry was obvious in the transverse and vertical dimensions • Cant of occlusal plane was apparent
	Max-Rev-Cant type (24.2%)	Group B (Ramus–Angle type, 16%) • Same ramus height difference between the deviated and non-deviated sides as group A • Menton was deviated in the opposite direction to shorter ramus	Group 3 (Atypical asymmetry, 12%) • Reverse maxillary canting • Deviation of the menton to the short side • Prominence of the angle/gonion on the larger side	Group 3 (26%) • Menton and ramus deviated in opposite directions, which seemed secondary to a yaw rotation
	Not matched	Group D (Bulkiness type, 28%) • Similar to group A • Small difference in magnitude		

Max-Cant, maxillary-cant; Man-Shift-Yaw, mandibular-shift and yaw; Max-Rev-Cant, maxillary reverse-cant; Ag, antegonion; U3, distance between Frankfort horizontal plane and midpoint of bracket slot of upper canine; U6, distance between Frankfort horizontal plane and midpoint of bracket slot of upper first molar; 3D-CT, three-dimensional computed tomography; PA, posteroanterior; CBCT, cone beam computed tomography.

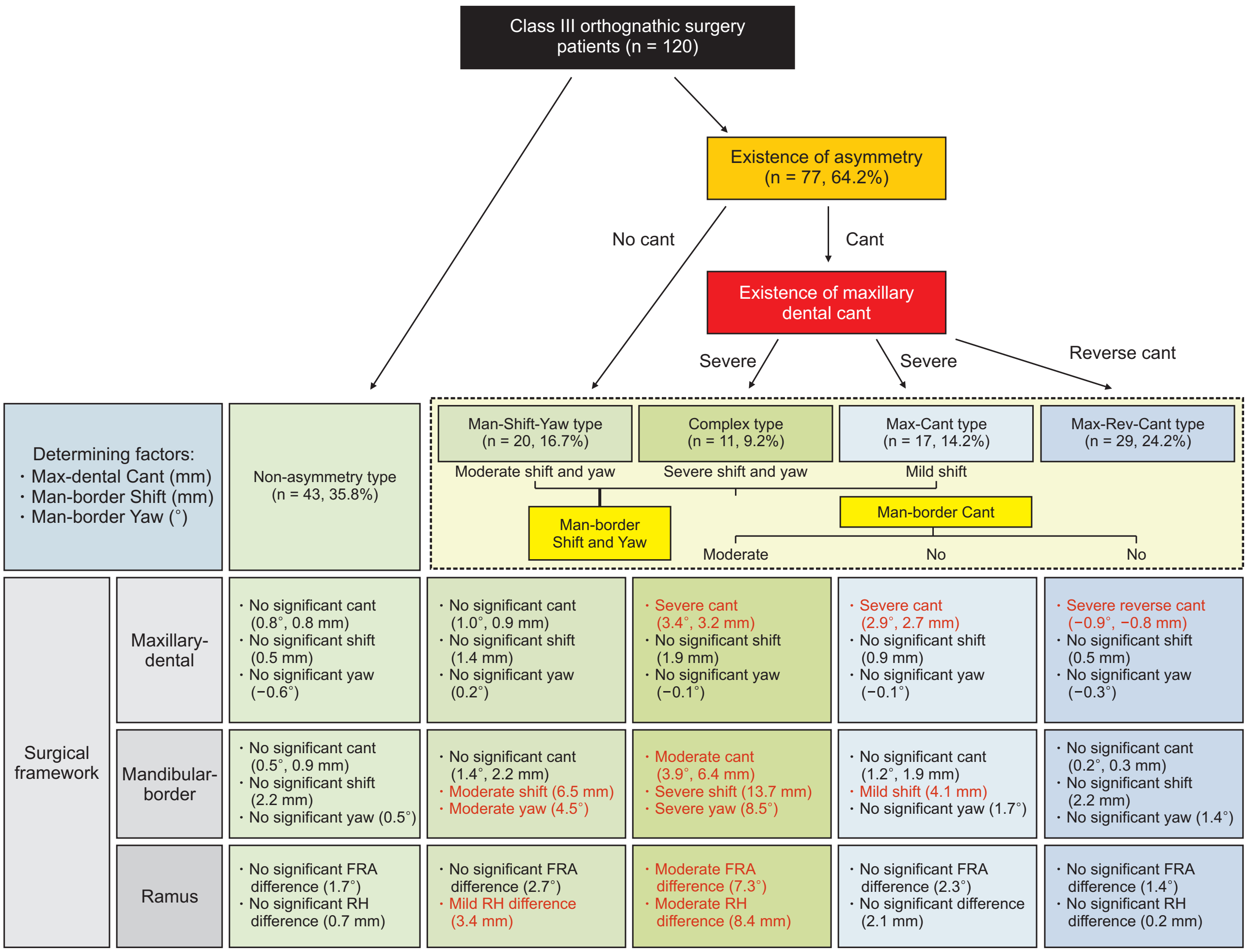

Figure 5. Flow chart that explains the characteristics of the facial asymmetry phenotypes in skeletal Class III patients who underwent orthognathic surgery.
Max-Cant, maxillary-cant; Man-Shift-Yaw, mandibular-shift and yaw; Max-Rev-Cant, maxillary reverse-cant; FRA, frontal ramus angle; RH, ramus height.

cant in the maxillary dentition may conceal the shift of the maxilla. Tay[20] suggested that unilateral mastication on the Me deviation side was related to this FA type.

Strategic decompensation according to the FA phenotypes (Figure 6)

Cant correction is required for the Max-Cant type, complex type, and Max-Rev-Cant type. Maxillary and mandibular molar height discrepancies less than 3 mm and 1.5 mm, respectively, can be treated by unilateral intrusion/extrusion of these teeth using miniscrews (known as a temporary anchorage device [TAD]) during pre-operative orthodontic treatment.[21,22] Then, the remaining molar height discrepancy and OP cant after pre-operative orthodontic treatment should be corrected by orthognathic surgery.

In the Man-Shift-Yaw type and the complex type, both transverse and horizontal decompensations are required to correct the shift and yaw in the mandibular dentition simultaneously. In terms of transverse decompensation of the molar inclinations, we can upright the posterior teeth on the basal arch and expand the inter-premolar width up to 4 mm and the inter-molar width up to 2 mm.[23] Then, we have to decide whether we should intentionally create the posterior crossbite on the deviated side and increase the amount of maxillary and mandibular dental midline-off for maximizing the surgical correction of the shift.

During horizontal decompensation, it is important to coordinate the dental and basal arch forms and correct the asymmetric molar relationship. Since the amount of distalization of the mandibular posterior teeth is considered to be 3 mm,[24,25] we can apply unilateral distalization of the mandibular posterior teeth in the deviated

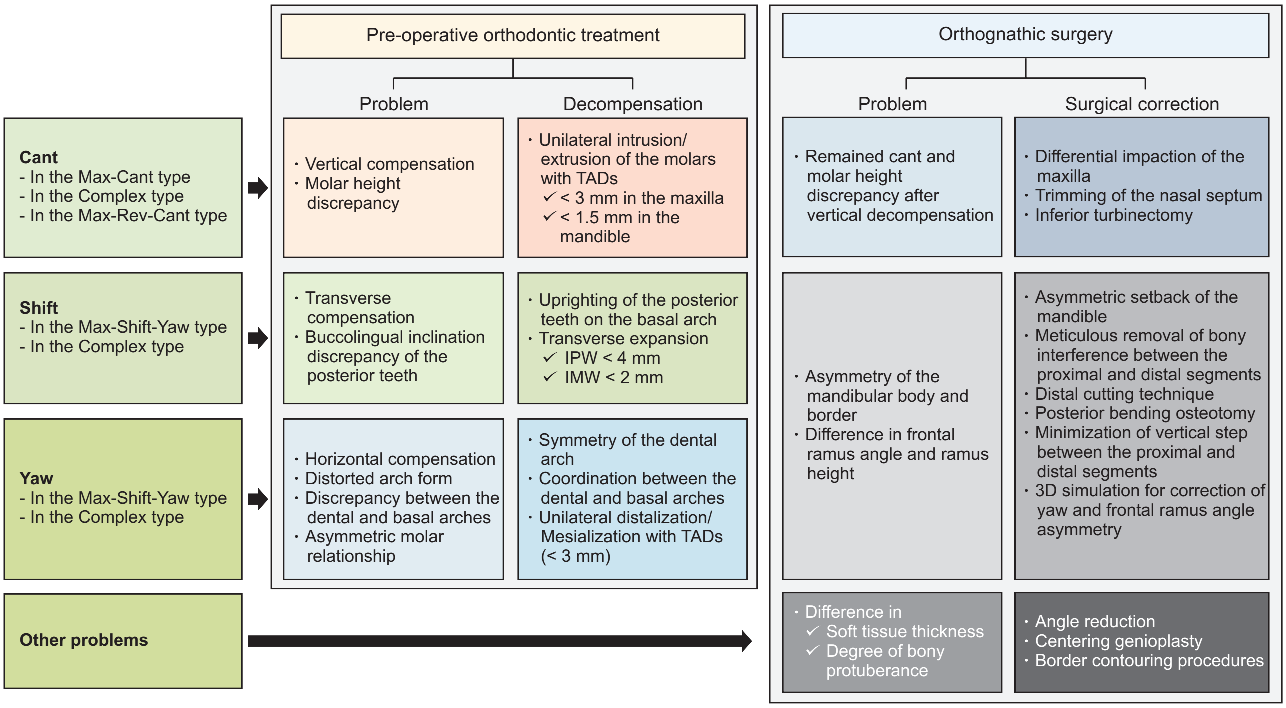

Figure 6. Strategic decompensation and surgical planning according to the facial asymmetry phenotypes.
Max-Cant, maxillary-cant; Man-Shift-Yaw, mandibular-shift and yaw; Max-Rev-Cant, maxillary reverse-cant; TAD, temporary anchorage device; IPW, inter-premolar width; IMW, inter-molar width; 3D, three-dimensional.

side up to 3 mm with TAD to maximize the surgical correction of the yaw.

Strategic surgical planning according to the FA phenotypes (Figure 6)

For correction of the remaining OP cant and molar height difference of the maxillary dentition after pre-operative orthodontic treatment in the Max-Cant type and the complex type, differential impaction of the maxilla can be performed. However, interference by the inferior nasal concha and nasal septum during impaction of the maxilla can result in deviation of the nasal septum and asymmetry of the nasal tip.[26] To prevent these adverse effects, trimming of the nasal septum and inferior turbinectomy can be considered.[26]

If the difference in the amount of mandibular setback between the deviated and non-deviated sides is large in the Man-Shift-Yaw type and the complex type, there is a high probability of bony interferences between the proximal and distal segments of the mandible. This can cause displacement and torque of the condyle, which is one of the main causes of post-surgical relapse. To prevent these problems, the following should be considered: (1) meticulous removal of the bony interference between the proximal and distal segments, (2) a distal cutting technique and/or posterior bending osteotomy of the distal segment, (3) minimization of the vertical step interference between the proximal and distal segments, and (4) 3D simulation to correct yaw and FRA asymmetry.[27-29]

When the patient has a large difference in the soft tissue thickness or the degree of bony protuberance of the mandibular border between the deviated and non-deviated sides, angle reduction, centering genioplasty, and border contouring procedures can be considered in conjunction with orthognathic surgery or as the secondary operation after orthognathic surgery.

This FA phenotype classification might be an effective tool for the differential diagnosis and for proper surgical planning of Class III patients with FA. Although this study provided meaningful results and compared the results with previous studies (Table 5), the morphology of the mandible was not analyzed in this study. In the future, it would be necessary to investigate the morphological abnormalities, such as hemimandibular elongation and hemimandibular hyperplasia.

CONCLUSION

• In the present study, the classification and percentage distribution of the FA phenotypes obtained from K-means cluster analysis were as follows: Non-asymmetry type (35.8%); Max-Cant type (14.2%), which showed severe cant of the maxillary dentition, mild shift of the mandibular border; Man-Shift-Yaw type (16.7%), which presented moderate shift and yaw of the mandibular border, mild RH-difference; Complex type (9.2%) with severe cant of the maxillary dentition, moderate cant, severe shift, and severe yaw of the mandibular border, moderate differences in FRA and RH; and Max-Rev-Cant type (24.2%), which showed reverse-cant of the maxillary dentition.

• Important measurement variables for differential diagnosis and a primary guideline of pre-operative orthodontic treatment and orthognathic surgery planning according to FA classification in Class III patients were also presented.

CONFLICTS OF INTEREST

No potential conflict of interest relevant to this article was reported.

ACKNOWLEDGEMENTS

This research was supported by a grant of the Korea Health Technology R&D Project through the Korea Health Industry Development Institute, funded by the Ministry of Health & Welfare, Republic of Korea (grant number: HI18C1638).

This article is partly from the PhD thesis of S.W.H.

REFERENCES

1. Cheong YW, Lo LJ. Facial asymmetry: etiology, evaluation, and management. Chang Gung Med J 2011;34:341-51.
2. Piao Y, Kim SJ, Yu HS, Cha JY, Baik HS. Five-year investigation of a large orthodontic patient population at a dental hospital in South Korea. Korean J Orthod 2016;46:137-45.
3. Bergersen EO. Enlargement and distortion in cephalometric radiography: compensation tables for linear measurements. Angle Orthod 1980;50:230-44.
4. Katsumata A, Fujishita M, Maeda M, Ariji Y, Ariji E, Langlais RP. 3D-CT evaluation of facial asymmetry. Oral Surg Oral Med Oral Pathol Oral Radiol Endod 2005;99:212-20.
5. Hwang HS, Hwang CH, Lee KH, Kang BC. Maxillofacial 3-dimensional image analysis for the diagnosis of facial asymmetry. Am J Orthod Dentofacial Orthop 2006;130:779-85.
6. Maeda M, Katsumata A, Ariji Y, Muramatsu A, Yoshida K, Goto S, et al. 3D-CT evaluation of facial asymmetry in patients with maxillofacial deformities. Oral Surg Oral Med Oral Pathol Oral Radiol Endod 2006;102:382-90.
7. Baek SH, Cho IS, Chang YI, Kim MJ. Skeletodental factors affecting chin point deviation in female patients with class III malocclusion and facial asymmetry: a three-dimensional analysis using computed tomography. Oral Surg Oral Med Oral Pathol Oral Radiol Endod 2007;104:628-39.
8. Akhil G, Senthil Kumar KP, Raja S, Janardhanan K. Three-dimensional assessment of facial asymmetry: a systematic review. J Pharm Bioallied Sci 2015;7(Suppl 2):S433-7.
9. Hwang HS, Youn IS, Lee KH, Lim HJ. Classification of facial asymmetry by cluster analysis. Am J Orthod Dentofacial Orthop 2007;132:279.e1-6.
10. Baek C, Paeng JY, Lee JS, Hong J. Morphologic evaluation and classification of facial asymmetry using 3-dimensional computed tomography. J Oral Maxillofac Surg 2012;70:1161-9.
11. Kim JY, Jung HD, Jung YS, Hwang CJ, Park HS. A simple classification of facial asymmetry by TML system. J Craniomaxillofac Surg 2014;42:313-20.
12. López DF, Botero JR, Muñoz JM, Cárdenas-Perilla R, Moreno M. Are there mandibular morphological differences in the various facial asymmetry etiologies? A tomographic three-dimensional reconstruction study. J Oral Maxillofac Surg 2019;77:2324-38.
13. Tyan S, Park HS, Janchivdorj M, Han SH, Kim SJ, Ahn HW. Three-dimensional analysis of molar compensation in patients with facial asymmetry and mandibular prognathism. Angle Orthod 2016;86:421-30.
14. Kim KA, Lee JW, Park JH, Kim BH, Ahn HW, Kim SJ. Targeted presurgical decompensation in patients with yaw-dependent facial asymmetry. Korean J Orthod 2017;47:195-206.
15. Chen YJ, Yao CC, Chang ZC, Lai HH, Yeh KJ, Kok SH. Characterization of facial asymmetry in skeletal Class III malocclusion and its implications for treatment. Int J Oral Maxillofac Surg 2019;48:1533-41.
16. Kwon SM, Baik HS, Jung HD, Jang W, Choi YJ. Diagnosis and surgical outcomes of facial asymmetry according to the occlusal cant and menton deviation. J Oral Maxillofac Surg 2019;77:1261-75.
17. Hong M, Kim MJ, Shin HJ, Cho HJ, Baek SH. Three-dimensional surgical accuracy between virtually planned and actual surgical movements of the maxilla in two-jaw orthognathic surgery. Korean J Orthod 2020;50:293-303.
18. Hwang HS, Thiesen G, Araújo TM, Freitas MP, Motta AT. An interview with Hyeon-Shik Hwang. Dental Press J Orthod 2016;21:24-33.
19. Joondeph DR. Mysteries of asymmetries. Am J Orthod Dentofacial Orthop 2000;117:577-9.
20. Tay DK. Physiognomy in the classification of individuals with a lateral preference in mastication. J Orofac Pain 1994;8:61-72.

21. Jeon YJ, Kim YH, Son WS, Hans MG. Correction of a canted occlusal plane with miniscrews in a patient with facial asymmetry. Am J Orthod Dentofacial Orthop 2006;130:244-52.
22. Takano-Yamamoto T, Kuroda S. Titanium screw anchorage for correction of canted occlusal plane in patients with facial asymmetry. Am J Orthod Dentofacial Orthop 2007;132:237-42.
23. Fleming PS, Lee RT, Mcdonald T, Pandis N, Johal A. The timing of significant arch dimensional changes with fixed orthodontic appliances: data from a multicenter randomised controlled trial. J Dent 2014;42:1-6.
24. Sugawara J, Daimaruya T, Umemori M, Nagasaka H, Takahashi I, Kawamura H, et al. Distal movement of mandibular molars in adult patients with the skeletal anchorage system. Am J Orthod Dentofacial Orthop 2004;125:130-8.
25. Yu J, Park JH, Bayome M, Kim S, Kook YA, Kim Y, et al. Treatment effects of mandibular total arch distalization using a ramal plate. Korean J Orthod 2016;46:212-9.
26. On SW, Baek SH, Choi JY. Quantitative evaluation of the postoperative changes in nasal septal deviation by diverse movement of the maxilla after Le Fort I osteotomy. J Craniofac Surg 2020;31:1251-15.
27. Baek SH, Kim TK, Kim MJ. Is there any difference in the condylar position and angulation after asymmetric mandibular setback? Oral Surg Oral Med Oral Pathol Oral Radiol Endod 2006;101:155-63.
28. Yang HJ, Hwang SJ. Change in condylar position in posterior bending osteotomy minimizing condylar torque in BSSRO for facial asymmetry. J Craniomaxillofac Surg 2014;42:325-32.
29. Ho CT, Lin HH, Liou EJ, Lo LJ. Three-dimensional surgical simulation improves the planning for correction of facial prognathism and asymmetry: a qualitative and quantitative study. Sci Rep 2017;7:40423.